An automated system for interrogating the evolution of microbial endosymbiosis

ARTICLE

An automated system for interrogating the evolution of microbial endosymbiosis

Can Huang[a+], Fengguang Guo[b+], Han Wang[c], Jasmine Olivares[b], James Dalton, III[b], Olga Belyanina[b], Alice R. Wattam[d], Clark A. Cucinell[d], Allan W. Dickerman[d], Qing-Ming Qin[b], Arum Han[a,e,f*], and Paul de Figueiredo[b,g*]

Inter-kingdom endosymbiotic interactions between bacteria and eukaryotic cells are critical to human health and disease. However, the molecular mechanisms that drive the emergence of endosymbiosis remain obscure. Here, we describe the development of a microfluidic system, named SEER (System for the Evolution of Endosymbiotic Relationships), that automates the evolutionary selection of bacteria with enhanced intracellular survival and persistence within host cells, hallmarks of endosymbiosis. Using this system, we show that a laboratory strain of *Escherichia coli* that initially possessed limited abilities to survive within host cells, when subjected to SEER selection, rapidly evolved to display a 55-fold enhancement in intracellular survival. Notably, molecular dissection of the evolved strains revealed that a single-point mutation in a flexible loop of CpxR, a gene regulator that controls bacterial stress responses, substantially contributed to this intracellular survival. Taken together, these results establish SEER as the first microfluidic system for investigating the evolution of endosymbiosis, show the importance of CpxR in endosymbiosis, and set the stage for evolving bespoke inter-kingdom endosymbiotic systems with novel or emergent properties.

Introduction

Endosymbiosis is a major force driving the evolution of life. It is now appreciated that mitochondria and plastids, the classical membrane-bounded organelles of eukaryotic cells, evolved from bacteria through endosymbiosis[1, 2]. Inter-kingdom symbiotic interactions have also been critical to the evolution and physiology of land plants. For example, *Rhizobia*, endosymbiotic bacteria that fix atmospheric nitrogen, provide critical nutrients to many crops of agricultural importance, including legumes[3]. In another example, *Wolbachia*, which encompass a large group of endosymbiotic bacteria, play central roles in supporting the lifestyle of Ecdysozoa species, including terrestrial arthropods[4, 5]. Finally, emerging

[a.] Department of Electrical and Computer Engineering, Texas A&M University, College Station, TX 77843
[b.] Department of Microbial Pathogenesis and Immunology, Texas A&M Health Science Center, Bryan, TX 77843
[c.] Department of Biomedical Engineering, School of Medicine, Tsinghua University, 100084, Beijing, China
[d.] Biocomplexity Institute and Initiative, University of Virginia, Charlottesville, VA 22904
[e.] Department of Biomedical Engineering, Texas A&M University, College Station, TX 77843
[f.] Artie McFerrin Department of Chemical Engineering, Texas A&M University, College Station, TX, 77843
[g.] Department of Veterinary Pathobiology, Texas A&M University, College Station, TX 77843
+ These authors contributed equally to this work.
* Co-corresponding authors
E-mail: pjdefigueiredo@tamu.edu
Electronic Supplementary Information (ESI) available: [details of any supplementary information available should be included here]. See DOI: 10.1039/x0xx00000x

intracellular bacterial pathogens of humans and animals must acquire novel traits to survive, persist, or replicate within mammalian host cells, including immune cells like macrophages[6, 7]. Despite the importance of such interactions, surprisingly little is known about their molecular mechanisms, in general, and the mechanisms by which bacteria evolve to gain the ability of surviving within eukaryotic host cells, in particular. This fact reflects, in part, the paucity of tractable experimental systems for the stepwise interrogation of emergent endosymbiotic interactions.

To address this limitation, several reports described the development of systems in which synthetic, engineered, or evolved endosymbiotic interactions were interrogated. For example, the plant pathogen *Ralstonia solanacearum* was engineered to carry a symbiotic plasmid containing nitrogen-fixation genes from *Rhizobium*. The engineered bacteria was shown to establish productive symbiotic interactions with plants[8] and to enable plant growth in the absence of nitrogen supplementation. Interestingly, serial passaging of these recombinant strains in plants gave rise to variants with further enhanced symbiotic properties, thereby demonstrating that synthetic symbiotic interactions can be evolved when appropriate selective pressure is imposed on systems[9]. Genetic engineering of *Saccharomyces cerevisiae* towards synthetic symbiosis with bacteria has also been achieved, thereby setting the stage for the molecular dissection of genes that drive the evolution of organelles of endosymbiotic origin (e.g., mitochondria) or intracellular bacterial parasites[10]. Finally, serial passaging of bacterial pathogens in macrophages or propagation in animal models has been used to interrogate the

Please do not adjust margins
Lab on a Chip
Page 2 of 14

evolution of virulence-associated adaptations[11-13]. These studies demonstrated the utility of laboratory models for evaluating mechanisms driving alterations in bacterial survival and fitness in the host.

Despite these advances, our current understanding of the molecular drivers of the evolution of *de novo* endosymbiotic interactions remains incomplete. Previous studies had shown that laboratory systems for the analysis of non-endosymbiotic evolution of a single bacterial species can provide important insights into fundamental biological mechanisms, including genome stability, metabolic regulation, and antibiotic resistance[14, 15]. In these systems, target bacteria were subjected to multiple rounds of mutagenesis, selection, and amplification, ultimately leading to the evolution of highly adapted strains. Importantly, the study of the evolution of antibiotic resistance, a trait which contributes to human disease by thwarting pharmacological intervention, has enabled the development of novel strategies for defeating resistance. Hence, the study of evolution of potentially pathogenic traits ultimately benefits countermeasure development. With these ideas in mind, we pursued a strategy to develop systems that enable the evolution of interactions between a laboratory strain of *Escherichia coli* (DH5a) and murine macrophages (J774A.1) to display hallmarks of inter-kingdom endosymbiosis and pathogenesis.

One of the major hurdles in laboratory studies that interrogate the evolution of inter-kingdom endosymbiosis is the necessity of repeatedly performing the manipulations required for bacterial evolution and adaptation, as only after many rounds of evolutionary steps can such a process give rise to the emergence of endosymbiotic hallmarks. Thus, even though such an evolutionary strategy can accelerate the identification of interesting inter-kingdom endosymbiotic interactions, the time-consuming and labor-intensive nature of these experiments has been a major bottleneck in the field. Cognizant that implementation of an evolutionary strategy would greatly benefit from the reduced hands-on time and increased reproducibility afforded by automation, we developed a microfluidic lab-on-a-chip system to repeatedly execute the requisite manipulations of cells and reagents.

Microfluidic lab-on-a-chip systems have the capability to precisely handle extremely small numbers of cells and reagents, and to conduct complex multi-step assays that are automated in a single microchip format[16-18]. Such systems have been extensively utilized for various microbial studies[19-21]. However, there have been limited descriptions of systems that support inter-kingdom interactions, and no system has been reported in which the evolution of bacterial species towards endosymbiosis is performed on-chip (**Table S1**). Here, we describe an automated microfabricated microfluidic system named SEER (System for Evolving Endosymbiotic Relationships) that performed sequential multi-step cell- and reagent-handling processes that drive the evolution of microbes to acquire enhanced capacities to survive intracellularly. Finally, we show how the application of the SEER system uncovered new single nucleotide polymorphisms (SNPs) in the *cpxR* gene[22], a component of the stress response pathway of cells, that

substantially contributes to intracellular survival, a hallmark of endosymbiosis and intracellular bacterial pathogenesis.

Results

Evolutionary assay design. The central hypothesis of this study was that a system in which an interaction between bacterial and mammalian cells in the laboratory that leads to evolution can provide insight into mechanisms of endosymbiosis. To better understand how endosymbiotic properties evolved during these multi-cellular interactions, we developed a two-component biological model system that included murine macrophages (J774A.1 or RAW264.7), which readily
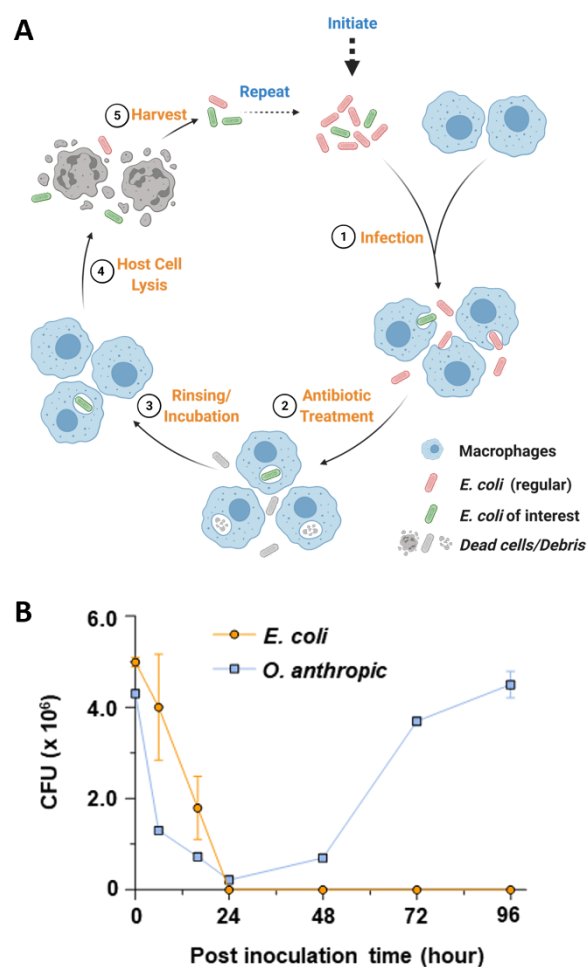
Figure 1. Evolutionary assay design. **A.** Proposed approach for analyzing the evolution of inter-kingdom endosymbiosis. Bacterial population is incubated with host cells for extended period of time, released from host cells, then reamplified in rich culture. Such steps can be performed repeatedly to acquire mutated strains with higher intracellular survival capability. **B**. Time-series intracellular survival of *Escherichia coli* and *Ochrobactrum anthropi* within host cells (macrophages) while applying the gentamicin protection regime. It can be seen that the intracellular *E. coli* population was efficiently killed, while *O. anthropi* population successfully survived within host cells and retrieved.

phagocytose bacteria, and *E. coli* (DH5α), a genetically tractable laboratory strain that initially showed limited intracellular survival in host cells. We designed a strategy to manipulate the inter-kingdom cellular system to promote the evolution of *E. coli* strains with enhanced intracellular survival and persistence (**Fig. 1A**).

To verify the utility of our strategy for measuring intracellular survival of bacteria, a laboratory strain of *E. coli* (DH5α) that displayed limited intracellular survival was first co-incubated with J774A.1 macrophage cells for 96 hours in the presence of gentamicin. Here, gentamicin was exploited because of its limited permeability across the plasma membrane of mammalian cells at low concentrations (e.g., 50 µg/mL). Therefore, gentamicin treatment in the evolutionary assay enabled the development of an *in vitro* method for killing extracellular bacterial populations while protecting their intracellular counterparts from harm[23]. Following host cell lysis, the number of viable intracellular bacteria that remained in the incubation chamber was analyzed. The result showed that gentamicin/host cell system efficiently killed the intracellular *E. coli* population. However, a positive control strain, *Ochrobactrum anthropi*, which replicates intracellularly, was efficiently recovered from infected host cells following

application of the gentamicin protection regime (**Fig. 1B**), as expected[24]. Taken together, these data establish a tractable biological system in which an analysis of the evolution of endosymbiotic properties could be performed, and in which repeated rounds of bacterial infection of host cells, incubation, and recovery of the internalized bacteria, could be used to study the evolution of endosymbiotic features.

Porous membrane-based microfluidic cell trapping and release system. We designed a lab-on-a-chip system that can mix, separate, and selectively retain two distinct cell types. The system was configured with two stacked milliliter-scale cell culture chambers with a porous polycarbonate membrane sandwiched in the middle. The membrane-based cell trapping method was selected because compared to the many different microfluidic-based cell manipulation methods (both passive and active methods), it is the easiest and most efficient system for selective cell trapping and release, as well as solution exchange. GFP-*S. enterica* and RAW264.7 macrophage were used to demonstrate the proper functionality of all the key cell and reagent manipulation steps required for the evolution assay (**Fig. 2**).

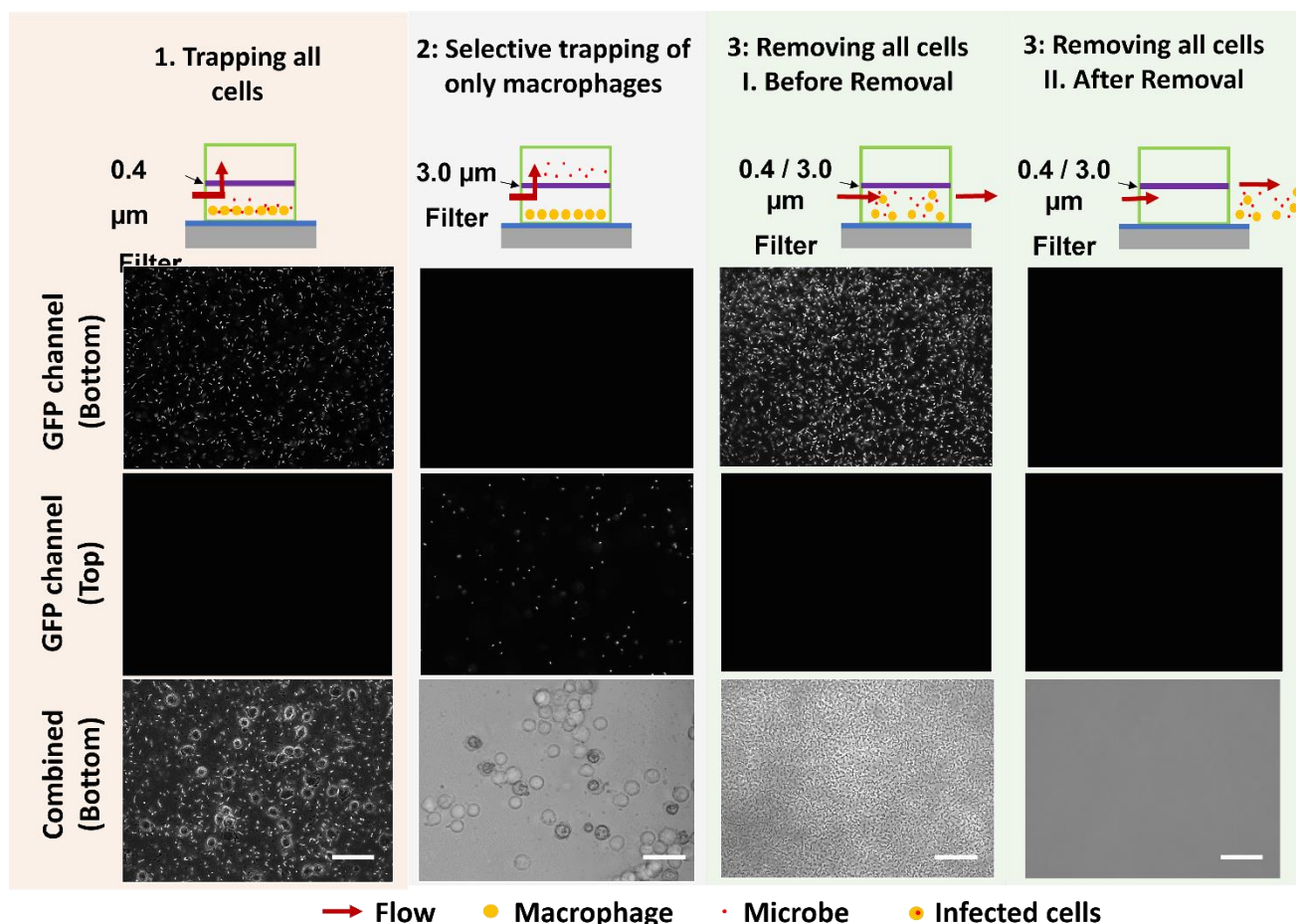**Figure 2.** Key functions of porous membrane-based microfluidics for selective trapping of macrophages and bacterial cells. Vertical flow through a 0.4 µm pore membrane can trap both types of cells; vertical flow through a 3.0 µm pore membrane can selectively trap mammalian cells while allowing bacterial cells to pass; lateral flow can rinse off both cell types from the microfluidic system. Scale bar: 50 µm.
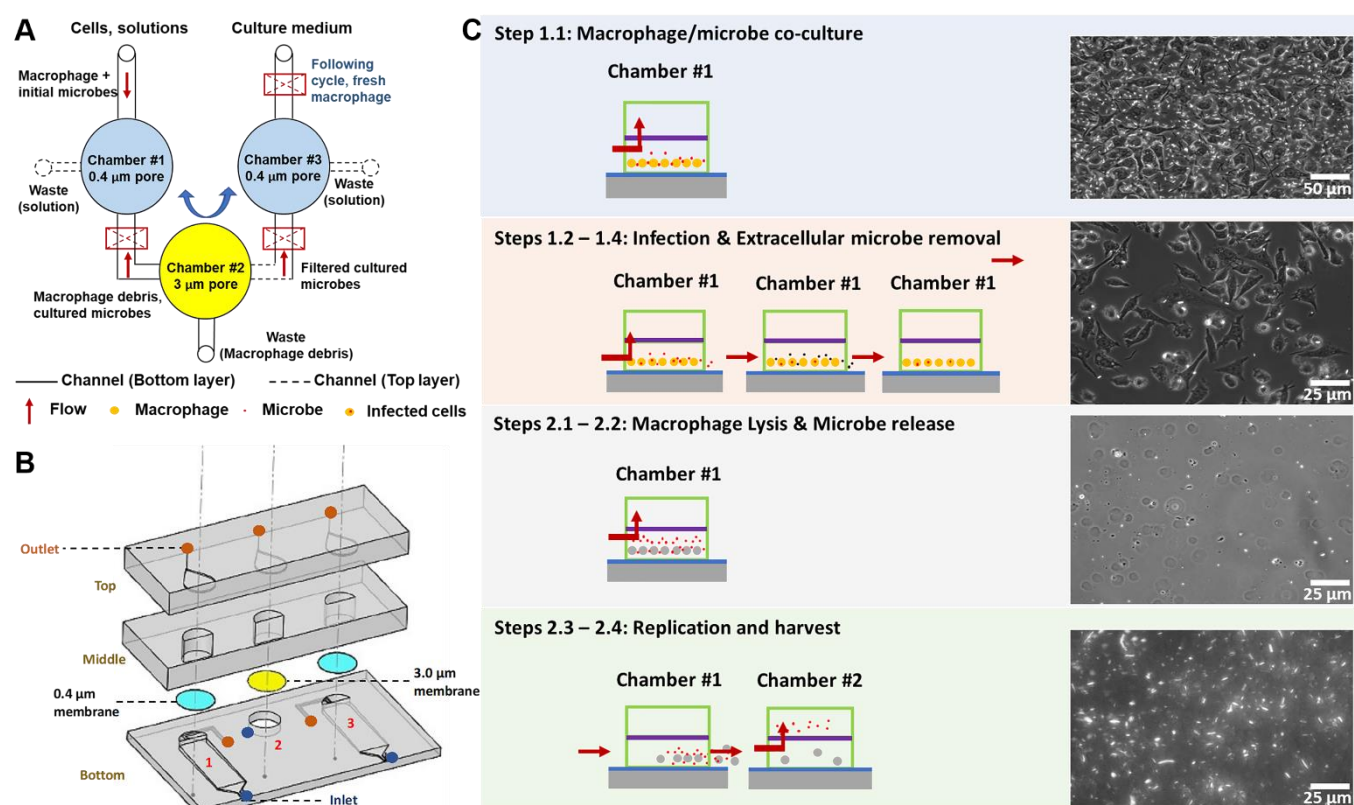
Figure 3. SEER platform configuration and validation. **A-B**. Interconnection of 3 porous membrane-based trapping units. **C**. Step-by-step functions of the porous membrane-based trapping unit achieved and validated using GFP-*Salmonella* cells and macrophages.

The integrated unit was configured with two fluidic ports (serve as one inlet and one outlet) at the bottom chamber and one fluidic port (one outlet) at the top chamber. This design enabled both vertical flow and lateral flow operations. When applying a vertical flow from the bottom chamber to the top chamber through the membrane with cellular contents of interest, this configuration selectively trapped either only the bigger cell type or both cell types, depending on the pore size of the membrane. For example, when host cells (10 – 15 μm size) and microbes (1.5 – 3.0 μm size) were used, applying a vertical flow carrying both cell types through a unit that was configured with a 0.4 μm pore membrane trapped both cell types in the bottom chamber, which enabled co-cultivation of the two cell types (**Fig. 2, step 1**). This configuration also allowed solution exchange as well as cell washing steps to be performed by simply flowing a different solution vertically through the same 0.4 μm pore membrane.

The washing and solution exchange steps were designed to satisfy the multiple intermediate steps in the integrated SEER system. When applying a vertical flow through a unit that was configured with the 3.0 μm pore membrane, only the host cells were physically blocked from exiting and were therefore trapped in the bottom chamber. However, the smaller microbes readily flowed through the membrane due to their smaller dimensions. This flow resulted in the selective trapping of only host cells in the chamber, which essentially achieved separation of the two cell types, where the top and bottom chamber will contain microbial cells and host cells, respectively. This trapping step was needed when washing out non-internalized microbes

after the cellular co-incubation reaction, or when harvesting the intracellularly surviving microbes at the end of each round of co-incubation (**Fig. 2, step 2**). Lastly, regardless of the pore size of the integrated membrane, when lateral flow was applied, all trapped cells were retrieved from the unit, or the device chamber could be cleaned for later re-usage (**Fig. 2, step 3**).

SEER microfluidic system design and validation. Upon the successful selective cell manipulation, we then performed several experiments to validate the functionality of the SEER system (**Fig. 3A**). Here, GFP-expressing *S. enterica* and RAW264.7 macrophages were utilized to visualize the dynamics of the bacterial populations during an evolutionary cycle. As shown in **Fig. 3B**, the basic unit has a top-bottom culture chamber with a porous membrane in between. Chamber #1 had a 0.4 μm pore membrane and was used to trap and co-incubate both microbes and host cells in the bottom chamber (**Fig. 3C step 1.1**). After applying lateral flow with buffer solution to remove the non-internalized bacterial cells, gentamicin-containing culture media was replenished into the system for long-term culture. Afterwards, another lateral buffer rinsing step was applied to remove the antibiotic-containing culture media and cellular debris stemming from the killed microbes (**Fig. 3C step 1.2 – 1.4**). At this moment, mammalian host cells were adherent to the bottom substrate; therefore, they were retained in the culture chamber during the lateral flow washing process. Then, lysis buffer was applied with vertical flow and host cells were lysed to release the intracellular bacterial population. The released bacteria were retained inside the
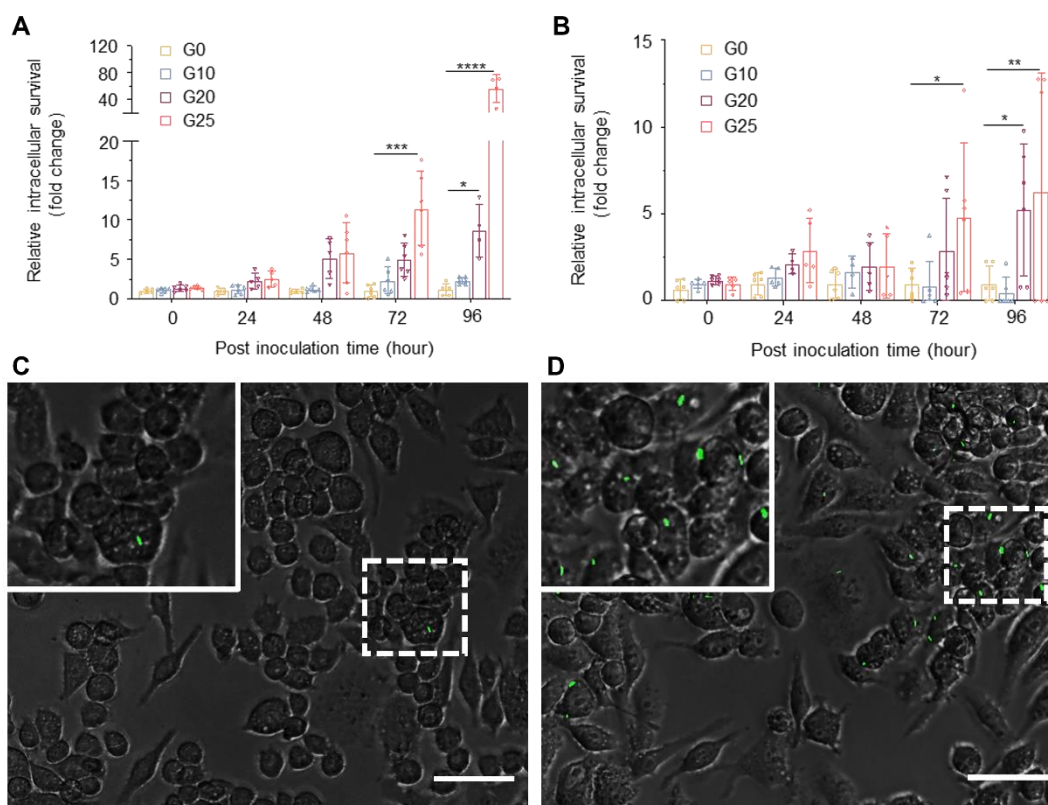
Figure 4. Post evolution harvest analysis. **A-B**. Relative intracellular survival of harvested strain from 2 independent series of evolution (25 rounds each). Both evolved G25 strains demonstrated increased survival capability when compared with naïve strain. **C-D**. Comparison of GFP-transfected survived naïve *E. coli* (C) and evolved G25 *E. coli* (D) at 96 h post inoculation (h.p.i.). Scale bar: 50 μm.

bottom chamber (**Fig. 3C step 2.1 – 2.2**). Next, rich culture media was vertically introduced into the system to facilitate bacterial amplification, and the total bacterial population was monitored until sufficient amplification had been achieved to support the next cycle of the evolutionary assay. Finally, the remaining material, which contains host cell, debris, and bacterial cells, was harvested by lateral retrieval, then immediately introduced into the second interconnected unit (Chamber #2) that contained a 3.0 μm membrane. In chamber #2, the harvested culture was passed vertically through the 3.0 μm membrane where the host cells and debris were blocked and retained in the bottom chamber, while bacterial populations passed through into the top chamber (**Fig. 3C step 2.3 – 2.4**). Finally, the filtered bacterial population was introduced into the third interconnected unit (Chamber #3) that was configured with a 0.4 μm pore membrane. Bacterial cells, as the starting material for the next cycle, was mixed with fresh host cells and then subjected to the next round of evolutionary selection. While the second cycle was being conducted and the third unit was being utilized for incubation, the first and second unit were treated with a sterilizing solution to be made ready for the next cycle in the device. The detailed assay steps are described in **Fig. S1**. The three-unit design allowed the evolving bacterial population to be transferred between two identical reaction chambers during repeated evolutionary cycles, and also enabled device sterilization (**Fig. S2**) without pausing the experimental workflow. We used a LabVIEW™ program that

controlled the syringe pump and pneumatically actuated microvalves to conduct the SEER-based evolutionary assay. The workflow diagram is included in the supplementary document (**Fig. S3**).

Evolved strain characterization. To investigate the dynamics of genomic alternations and to find out their underlying correlations with phenotypic changes seen in the SEER-evolved strains, we performed 25 rounds of bacterial internalization into host cells, incubation of the infected host cells for various lengths of time, recovery of the surviving internalized bacterial cells, and amplification of the recovered cells. The 25-round selection process was conducted twice independently to enable cross comparison of evolutionary trajectories. Samples of the intermediately evolved populations were collected and designed as EcG0-1 to EcG25-1, and EcG0-2 to EcG25-2, respectively, where "Gxx" stands for the corresponding evolutionary cycles that has been completed when such sample was harvested from the evolutionary assay.

These harvested strains were examined with various biological assays to identify phenotypes that differed from their naïve counterparts. First, we tested the relative intracellular survival of the parental and evolved strains at 1 h and 96 h post-inoculation (h.p.i.). A maximal 55-fold increase in intracellular survival of the evolved strains were observed at 96 h.p.i. (**Fig. 4A, 4B**), with increasing levels of intracellular survival observed as the rounds of evolutions increased (from G0 to G10, G20, and

Please do not adjust margins
Lab on a Chip
Page 6 of 14

Table 1: Identified changes in functional genes. The percentage of each specific mutant gene presented in each evolved population (N = 8) were calculated in the last 3 columns. *Note: * N/A means the gene name is not available; bold highlights indicate the mutation accumulated as the microbe evolved from G0 to G25.*

Gene Name*	Gene Description	Protein change	Mutation type	G10	G20	G25
ybfC	Uncharacterized protein	Lys189fs	Deletion	37.5	0	0
ygcQ	Electron transfer flavoprotein, alpha subunit YgcQ	Leu220Arg	Nonsynonymous	50	0	0
tus	DNA replication terminus site-binding protein	Pro160Thr	Nonsynonymous	100	62.5	100
N/A	core protein	Gln33Lys	Nonsynonymous	12.5	0	12.5
N/A	core protein	Gln33Lys	Nonsynonymous	87.5	75	75
rhsA	**Protein RhsA**	**Ala179Thr**	**Nonsynonymous**	**0**	**12.5**	**25**
rhsA	Protein RhsA	Lys262Thr	Nonsynonymous	0	12.5	12.5
cpxR	**Copper-sensing two-component system response regulator**	**Gly89Ala**	**Nonsynonymous**	**0**	**25**	**87.5**
cpxA	Copper sensory histidine kinase	Val174Ala	Nonsynonymous	0	50	0
cpxA	**Copper sensory histidine kinase**	**Arg191His**	**Nonsynonymous**	**0**	**62.5**	**87.5**
N/A	FIG01269488 protein, clustered with ribosomal protein L32p	Gln154Leu	Nonsynonymous	100	87.5	87.5
csgA	Major curli subunit precursor	Val118Phe	Nonsynonymous	100	87.5	87.5
yiaA	Inner membrane protein YiaA	Ala88Thr	Nonsynonymous	25	0	0
mtlA	PTS system, mannitol specific EIIABC component	Ser26Phe	Nonsynonymous	50	0	0
N/A	Ferric hydroxamate outer membrane receptor FhuA	Val1_Leu2insValProLeu	Insertion	25	12.5	12.5
pinQ/pinR	Serine recombinase, PinQ/PinR-type	Ala159Val	Nonsynonymous	50	50	37.5
pinQ/pinR	Serine recombinase, PinQ/PinR-type	Arg3Gln	Nonsynonymous	50	37.5	25
ynaE	Uncharacterized protein, YnaE family	Thr51Lys	Nonsynonymous	62.5	50	50
gadA/B	Glutamate decarboxylase (EC 4.1.1.15)	Lys1_Asn2insAspLeuSerIleAsnLys	Insertion	12.5	0	25
N/A	core protein	Lys189fs	Insertion	0	12.5	12.5

G25). The differences in intracellular survival were also confirmed by comparing microscopy images of the GFP-labeled parental strain with corresponding images of the evolved strains following co-incubation with macrophages (**Fig. 4C, 4D**). Second, we tested the growth rate of the naïve and evolved strains when grown in various liquid culture media. We noted that the evolved bacteria displayed no differences in growth rates in minimal (M9 with 0.2% glucose) and rich (LB) media compared to naïve controls. Finally, we tested the antibiotic, acid, and oxidative stress sensitivities of the naïve and evolved strains. We found that the evolved strains displayed resistance to these stresses (**Table S2**), suggesting that this phenotype may account for enhanced intracellular survival, at least partially. Moreover, the enhanced survival was correlated with enhanced resistance to stresses that bacteria were expected to encounter inside host cells. Additionally, when testing the sensitivity of the evolved strains against various types of antibiotics, we found that the evolved strain developed low levels of resistance to gentamicin (1.25 µg/mL). However, under the experimental conditions (50 µg/mL), both naïve and evolved strains did not survive (**Fig. S4**). This finding indicates that the selection protocol, which utilizes gentamicin to kill extracellular microbial populations, remained effective even after 25 rounds of evolution. Taken together, this data demonstrates that the surviving population of *E. coli* strains did not arise as a consequence of evolved resistance to gentamicin, and moreover, establishes the functionality of our evolutionary assay.

Identification of gene mutations. To determine the specific mutations that conferred enhanced intracellular survival, we sequenced and then aligned the genomes of the naïve strain against two sets of independently SEER-evolved strains. A total of 203 single nucleotide polymorphisms (SNPs) were identified (**Table S3**). After removing from further consideration variants that appeared only in a single read, encoded synonymous SNPs, or were in intergenic regions, RNA genes, or occurred in genes associated with bacteriophages, transposases, or mobile element proteins, we were left with a total of 20 non-synonymous SNPs or indels, which were considered candidates for mediating the observed phenotypic changes (**Table 1**).

***cpxR* mutation promotes *E. coli* survival in J774A.1 macrophage.** We hypothesized that mutations that benefit bacterial intracellular survival will be preferably represented in the evolved population. To test this possibility, we analyzed all 20 mutations in G10, G20, and G25 strains and found three SNPs in the *cpxR*, *cpxA*, and *rhsA* genes that were enriched in G25 strains. Mutations in two genes in the copper-sensing two-component system displayed the highest levels of enrichment in G25, and mutations in one of these genes (*cpxR*) that resulted in a single amino acid change (G89A) and accumulated in G20 (25% of all reads) and G25 (87.5% of all reads) (**Fig. 5A, 5B, Table 1**), were chosen for further study.

CpxR is a member of the two-component regulatory system CpxA/CpxR, which is known to respond to envelope stress responses, such as heat shock, high pH, oxidative stress, and nutritional deprivation, by activating the expression of downstream genes[22]. To test if the observed SNP in *cpxR* did
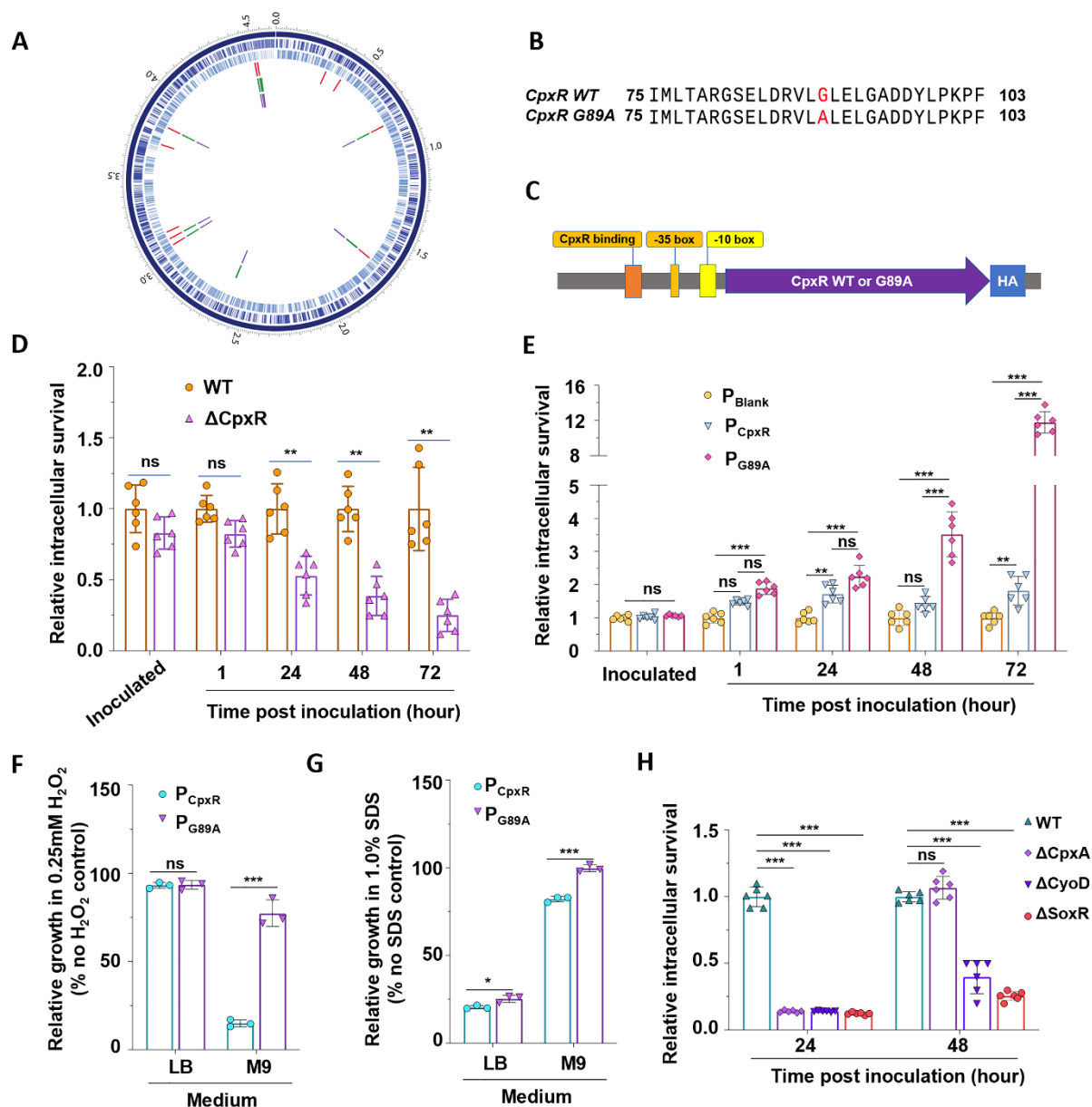
Figure 5. CpxR is critical for *E. coli* survival in J774A.1 macrophages. **A.** A circular diagram showing important SNPs in G10 (Red), G20 (Green), or G25 (Purple) comparing to G0. **B.** An SNP causes the change of amino acid from glycine to alanine at position 89 of the CpxR protein. **C.** Schematic of CpxR WT or G89A (CpxR mutant) expression cassette containing all engineering components. **D.** CpxR knockout strain (*ΔcpxR*) had lower survival rate in J774A.1 macrophages compared to wild type (WT) at 24, 48, and 72 h.p.i.. **E.** Bacteria carrying *cpxR* mutant plasmid (P_{G89A}) had higher survival rate than the one with wild type *cpxR* plasmid (P_{CpxR}) in J774A.1 macrophages at 48 and 72 h.p.i., and P_{CpxR} strain also showed higher survival rate than the CpxR knock-out strain carrying a blank plasmid (P_{Blank}). **F.** P_{G89A} displayed better growth in SDS and H_2O_2 stress condition than P_{CpxR}, especially in M9 minimal medium. **G.** Stress-related genes, *cpxA*, *soxR*, and *cyoD*, play important role in *E. coli* intracellular survival. The survival rate in J774A.1 is significantly decreased at 24 h.p.i. for *cpxA* knockout *E. coli*, and at 24 and 48 h.p.i. for both *soxR* and *cyoD* knockout *E. coli* strains.

indeed control bacterial intracellular survival, we generated *cpxR* gene complementation strains that ectopically expressed either the wild-type *cpxR* allele (P_{WT}) or the *cpxR* G89A mutant (P_{G89A}) under the control of the *cpxR* promoter (**Fig. 5C**). The expression of CpxR and CpxR-G89A proteins was confirmed by Western blot using anti-HA tag antibodies (**Fig. S5B**). Additionally, the growth rates of the P_{WT} and P_{G89A} strains in LB medium were similar (**Fig. S5C**). We first found that the *cpxR*

knock-out strain (*ΔcpxR*) had lower survival rates in J774A.1 macrophages compared to that of wild type (WT) bacteria at 24, 48, and 72 h.p.i. (**Fig. 5D**). Furthermore, the P_{G89A} strain showed enhanced survival in host cells at 1, 24, 48, and 72 h.p.i. (**Fig. 5E**), thereby demonstrating that the G89A mutation in CpxR was indeed necessary and sufficient to improve the intracellular survival of the bacterium.

***CpxR* mutant displays resistance to other stresses.** CpxR controls various bacterial stress responses. To investigate if the CpxR mutation (G89A) contributed to such responses, we tested the growth of P_{WT} and P_{G89A} strains in rich (LB) and minimal (M9 with 0.2% glucose) media containing H_2O_2 or the detergent sodium dodecyl sulfate (SDS). The P_{G89A} strain showed better growth than its WT counterpart P_{WT} under both conditions. Specifically, LB and M9 medium containing 0.25 mM H_2O_2 had no effect on P_{G89A} growth, but the growth of the P_{WT} strain was significantly inhibited in M9 medium containing 0.25 mM H_2O_2 (**Fig. 5F**). In LB or M9 media containing 1 % SDS, the growth of the P_{WT} strain was inhibited in both media, whereas the growth of P_{G89A} was only partially suppressed in LB medium (**Fig. 5G**). To test if other stress-related genes were also important for bacterial intracellular survival in J774A.1 macrophages, we examined this phenotype in *E. coli* strains[25] harboring deletions in *cpxA* (encoding a sensor histidine kinase, an envelope stress response gene)[26], *soxR* (encoding a redox-sensitive transcriptional activator), or *cyoD* (encoding a cytochrome oxidase subunit IV, a component of SoxR regulon)[27]. Knocking out each of these genes resulted in dramatic decreases in the *E. coli* intracellular survival (**Fig. 5H**), showing that these three stress-related genes also play important roles in bacteria survival in macrophages.

Discussion

Microfluidic systems have generated enormous interest as tools for advancing the interrogation of biological systems at high throughput[28]. Recently, sophisticated systems that support the cultivation and growth of inter-kingdom interactions have been described, including in tissue mimetic models of the gut where microbial components contributed to appropriately modeling the physiology and function of this organ system[29]. However, despite this success, examples of devices that support the evolution of endosymbiosis have not been described. In this report we developed and demonstrated the utility of SEER, a microfluidic system that facilitates the analysis of the evolution of endosymbiotic features in bacteria. Endosymbiotic systems are prevalent in nature. However, mechanisms by which endosymbiotic systems emerge remain poorly understood, mainly due to the limited availability of experimental tools for such studies. The SEER system will help address this limitation by providing a facile platform in which the stepwise evolution of microbes with enhanced intracellular survival (a hallmark of endosymbiosis) as well as other features can be investigated.

The use of SEER system to interrogate the evolution of endosymbiotic features in bacteria resulted in several striking findings. First, we were surprised to observe that the enhanced intracellular survival of *E. coli* emerged rapidly. After 25 rounds of directed evolution in the SEER system, a 55-fold increase in intracellular survival was seen. These data not only reflect the stringent conditions under which the selection was performed, but also suggest that relatively few mutations were required to change the physiology of the naïve strain in a way that enhanced its intracellular survival. In this regard, the fact that we used a disarmed laboratory strain (*E. coli* DH5a) as starting

material for the directed evolution endeavor meant that small changes in the genome were sufficient to realize dramatic improvements in intracellular survival. We hypothesize that if a strain that was better adapted to the harsh intracellular environment of host cells was used for these studies, similar levels of improvement would not have been observed without many more rounds of selection. Future work using the SEER system will test this hypothesis.

Second, it is notable that the SEER-selected bacterial strains that displayed enhanced intracellular survival possessed mutations in the CpxR/CpxA system, a two-component signal transduction system that controls how bacteria perceive and respond to periplasmic stress, including misfolded proteins, inner membrane disruption, starvation, and high osmolarity[30-32]. Besides many stress response roles, the CpxA/CpxR system is also involved in the virulence of uropathogenic *E. coli* and *Salmonella enterica*, and the antibiotic resistance of *E. coli*[33] (**Table S4**). We detected 20 synonymous mutations or indels in the genome of the evolved strains when compared to the parental *E. coli* strain. Among the 20 mutations, two occurred in the CpxR/CpxA system (both G20 and G25). These findings demonstrated that the CpxR/CpxA system plays critical roles in *E. coli* intracellular survival. In addition, our findings showed that the single amino acid mutation (G89A) observed in adapted strains control *E. coli* survival by enhancing its stress tolerance.

Finally, it has become recently appreciated that the suppression or evasion of innate immune defense constitutes an important component of intracellular symbiotic or parasitic interactions[34]. These immune evasion pathways include the synthesis and delivery of effector proteins into host cells[35], alterations in membrane structures[36], and changes in rRNA sequences[37], which collectively inactivate or elude host immune defenses. We did not observe the acquisition of such immune evasive traits in our studies. For example, because *E. coli* does not contain a Type III or Type IV secretion system, the delivery of effector molecules to host cells through such secretion systems could not account for the observed enhanced intracellular survival.

Several aspects of the SEER microfluidic system merit consideration. First, the physical dimension of the pores in the membrane filters in the SEER system were utilized to achieve size-based separation of bacterial and mammalian cells. This configuration provided the highest throughput with the lowest system complexity when compared to other extensively studied microfluidic cell separation methodologies (e.g., dielectrophoresis[38, 39], acoustophoresis[40], hydrodynamics[41]). Additionally, the use of simple-to-microfabricate polydimethyl siloxane (PDMS) and the commercially available polycarbonate membrane filters not only enabled cost-effective fabrication options for broad laboratory applications, bult also design flexibility. Finally, the automated system can be operated with minimal manual input and could potentially reduce most operational errors, which in result enables the standardized repetitive investigations and tracking of the evolution trajectory throughout long-term experiments.

Resistant strains could in principle grow slower compared to sensitive strains, and therefore could potentially lose

dominance during the cultivation step. To precisely evaluate how this reproliferating step would affect the SEER selection efficiency, we picked three isolated colonies representing evolved and naïve strains. We then measured the growth of these strains in LB media for 16 hr (**Fig. S6**). As can be seen from the growth curve, the doubling time before/after 25 rounds of selection did not change much. Thus, in this case, the sensitive strain did not dominate the population during cultivation in rich media. However, in cases where the SEER system needs to be operated to achieve long-term evolution, replacing the cultivation step with intracellular cultivation would potentially help accelerate the overall population to shift towards endosymbiosis favouring adaptations – however, considering the additional pressure that evolved bacteria cells will be facing from co-cultivating with macrophages, such evolution of reproliferating bacteria may take a much longer time to reach the desired number of cells to continue to the next round of evolution.

The described development and utilization of the SEER platform enables a variety of exciting future directions. First, additional mutagenesis steps can be introduced between the evolutionary cycles to accelerate and diverse the mutations. Specifically, under certain circumstances where enhanced rates of mutagenesis are desired, ultra-violet or chemical treatment of bacterial cells can also be integrated into the system. Specifically, components that support induced mutagenesis could be embedded into the final amplification step at the top chamber of the second unit. A fully automated system can also be deployed to further extend the number of selection cycles while keeping human labor inputs at a minimal level. Second, although the SEER system was developed as a stand-alone unit, we envision that improvements made to the SEER system in the future will allow operating many chips in parallel, thereby allowing multiple lines of evolution to be conducted in parallel. Such parallelism could provide better reproducibility when a single biological system is deployed, or alternatively, enable diverse cellular models to be investigated at the same time (for example, different bacterial cells with various types of hosts). Third, in this report, 25 evolutionary cycles were sufficient to select strains that displayed substantially enhanced intracellular survival. However, in future work the number of evolutionary cycles can be increased to enable the *de novo* evolution of inter-kingdom interactions that display enhanced persistence. Finally, our work evolved a single bacterial strain in the SEER system. However, the system can also support evolutionary strategies where mixed bacterial communities are used, thereby creating the possibility for genetic exchange between community members. Such a community-based strategy could potentially increase the genetic diversity of individual strains, and thereby promote the emergence of novel evolutionary outcomes. Future work will be directed toward exploring this and other possibilities.

Experimental

Device design. The detailed dimensions of the entire microfluidics system are illustrated in **Fig. S7**. Here, chamber #1 and chamber #3,

which are mainly used during the co-incubation steps, are designed to have a volume of 800 µL to mimic the volume of a single well of a conventional well-plate. The surface area of the bottom chamber was also intentionally designed to be as large as possible to enable more host cells to be seeded on the glass substrate after the cell loading step. Because of the relatively large chamber size, issues associated with air bubbles clogging these large fluidic chambers are highly likely. Therefore, the chamber was designed to have a sloped ceiling (5° slope, **Fig. S7B**) so that any air bubbles accidentally introduced into the chambers will float upwards towards the membrane due to its buoyancy and then be released through the top outlet[42]. Chamber #2 mainly serves as a filtration and bacterial culture chamber, therefore was designed to have a smaller volume (200 µL).

Device fabrication. To fabricate the microfluidics device, a high-resolution 3D printer (Envision One) was first utilized to print out the master mold for the polydimethyl siloxane (PDMS) soft lithography process. The printed master mold was baked and cured under UV light overnight to fully cure the 3D printing resin. Liquid-phase PDMS (Sylgard 184 Dow Corning, MI, USA, base and curing agent mixed at 10:1) was poured onto the 3D-printed master mold and cured for 4 h at 65°C, and then released from the master mold. Following, the PDMS layers were treated with O_2 plasma and the bottom PDMS layer was bonded to the glass substrate immediately afterwards. Next, the filter membranes (Isopore Membrane Filter, HTTP04700, MilliporeSigma, USA) with different pore sizes were trimmed and glued with liquid PDMS onto the top of the bottom PDMS layer, and sandwiched by the second PDMS stacking layer to create each functional unit. After the final PDMS layer was bonded, the entire device was baked at 85°C for 30 min. Before experiment, the entire device was rinsed with ethanol and then autoclaved for sterilization.

Cell preparation. J774A.1 (ATCC TIB67) or RAW 264.7 (ATCC SC6003) macrophages were thawed and grown on cell culture flasks filled with DMEM containing 10% FBS at 37°C and a 5% CO_2 atmosphere. Macrophage cells were detached by a cell scraper prior to experiments and their concentration determined by a hemocytometer. Total number of macrophages injected into the microdevice were adjusted to 2 x 10^5 cells to reach an estimate confluency of 70% after seeding. *Salmonella enterica subsp. enterica* (ATCC 14028) cells engineered with GFP plasmid (pCM18) were inoculated from a single colony and cultured in Lysogeny Broth (LB, GeneMate, USA) medium with 50 µg mL^{-1} erythromycin at 37°C for 8 h. *E. coli* (DH5α, Thermo Fisher Scientific) strain was inoculated on an LB agar plate, and a single colony was picked and cultured in LB medium overnight. Right before experiments, the bacteria culture was centrifuged and washed with 1 x PBS (pH 7.4, unless otherwise indicated). The cell suspension was adjusted to OD of 1.0, and the total number of bacterial cells were adjusted to 2 x 10^6 to achieve a multiplicity of infection (MOI) of 10.

Operations of the on-chip evolutionary assay. Bacterial cells and host cells were initially mixed at an MOI of 10 and loaded into the chamber #1 with DMEM as carrier medium using a syringe pump. The infusion rate was set as 1 mL/h for 1 h, and the inlet at the

Please do not adjust margins
Lab on a Chip
Page 10 of 14

bottom chamber as well as the outlet at the top chamber were opened during the loading process. After cell loading, the system was incubated at 37°C for 1 h to allow host cell attachment on the bottom glass substrate. Next, PBS was introduced into the system as a lateral flow at 1 mL/h for 30 min to rinse off the excessive extracellular microbes. Following, the system was replenished with gentamicin-containing DMEM (Lonza, 17-518L, USA, at 50 μg/mL) culture medium at 1 mL/h for 45 min with a vertical flow format, and then further incubated at 37°C. The length of this incubation step was extended gradually as the evolutionary assay repeated, starting from 1 h to maximum 72 h. Afterwards, PBS at a flow rate of 3 mL/h was infused in lateral flow format to rinse off gentamicin and dead microbe residuals. Following, lysis buffer (2% Tween 20 in DI water) was infused in vertical flow format at 1 mL/h for 30 min, and the system was incubated at 37°C for 30 min. Next, PBS buffer was injected in vertical flow direction at 1 mL/h for 30 min to rinse off the lysis buffer, and then LB medium was injected at 1 mL/h for 30 min in lateral flow format to retrieve all released intracellular microbes and guide them into chamber #2. Within chamber #2, bacterial cells mixed with host cell debris were loaded in vertical flow format, and therefore all host cell debris were blocked and separated from the target bacterial cells harvested. Following, chamber #2 was incubated at 37°C inside a shaking incubator to amplify the population. Finally, the harvested bacterial cell population was retrieved from chamber #2 with PBS, sampled for stocking and off-chip confirmation purposes, and guided to chamber #3 to initiate the second round of evolutionary assay. In all the following cycles, the host cells were pre-seeded onto the glass substrate with a total population at 2×10^5 before the introduction of bacterial population.

While the evolutionary assay was ongoing in one of the incubation chambers (chamber #1 or chamber #3), the other two chambers that potentially has some cell residuals from previous round were rinsed with Proteinase K (in 1 x PBS, pH = 7.4, at 1:200), incubated, and rinsed with 70% ethanol, then PBS flown through at a flow rate of 3 mL/h for 30 min to fully clean any remaining residues (**Fig. S2**).

Characterization of endosymbiosis phenotype. To validate the phenotypic changes occurring along with the evolutionary selection process, six single colonies each picked at G0, G10, G20, G25 stages were characterized with plate assays and cross-compared. First, host cells (J774A.1) with a total number of 2×10^5 cells/well were loaded into a 24-well plate and seeded overnight. For each picked bacterial colonies, bacterial cells were inoculated and cultured in LB medium overnight and adjusted to OD 1.0 the following day. Bacterial cells were added into the well at 2×10^6 cells/well to keep the MOI to 10. After bacterial cell loading, the mixture was incubated with antibiotic-free DMEM at 37°C for 1 h to allow bacterial internalization into host cells. Following, host cells were rinsed with PBS thoroughly and culture medium was replaced to gentamicin-containing DMEM (50 μg/mL). At 0, 24, 48, 72 and 96 h.p.i., host cells were rinsed with PBS, then lysed with 2% Tween 20 lysis buffer. Released bacterial cells were plated on agar plates for colony forming unit (CFU) analysis to quantify the degree of survival of such strains at different time points and its relative survival phenotype when compared with the naïve strain. To visualize such

differences, colonies harvested at G25 were also engineered to express fluorescence and compared with G0. Microscopic images taken at different h.p.i. were also compared (**Fig. 4C, D**).

Bacteria Genome sequencing. Total DNA was extracted from 28 single colony isolates using the Quick-DNA™ Fungal/Bacterial Kits, which represents 4 isolates from G0, and 8 isolates from each of G10, G20, and G25. DNA integrity was checked using the Agilent TapeStation Genomic DNA tape and the amount of DNA quantified with the Qubit High Sensitivity dsDNA assay. All samples were normalized to the same input quantity and prepared for sequencing using the Bioo Scientific's Nextflex Rapid DNA-Seq library preparation kit with enzymatic fragmentation following the manufacturer's protocol. Samples were individually barcoded and then pooled in equimolar concentrations for sequencing on an Illumina MiSeq v3 2x300 sequencer.

Genome Assembly and Annotation. The quality of the reads was assessed using the FastQC[43] program available in the Pathosystems Resource Integration Center (PATRIC)[44]. These were assembled using SPAdes[45] 3.10.0 in the pipeline provided by PATRIC, which had the minimum contig coverage set a 5 and the minimum contig length set at 300 bp. The resulting contigs were annotated using the RASTtk pipeline[46], which is also available in PATRIC. This pipeline includes estimation of genome quality, completeness, and contamination.

Variant Analysis. Genome of *E. coli* G0 was used as the reference to compare the reads from eight isolates representing each of the three generations (G10, G20, and G25). The "Variation Service" in PATRIC was used in the analysis. Bowtie2[47] was selected as the aligner and FreeBayes[48] as the SNP caller. This service can identify and annotate sequence variations, including SNPs, SNVs (single nucleotide variants), and indels. Protein families[49] for each of the genes that had non-synonymous mutations in functional genes were identified.

Identifying homologs in known DH5α genome. To identify homologs in a known GenBank genome, the Proteome Comparison tool[50] at PATRIC was used. The *E. coli* strain DH5α (PATRIC genome ID 562.28198, GenBank genome ID CP026085) was used as the reference, and the proteins in this genome were compared by the bidirectional BLASTP[51] analysis provided by this tool with the S5 G0 genome. Homologs and the corresponding GenBank protein identifier in the reference genome were noted.

***cpxR* gene cloning and G89A site mutation.** *cpxR* gene with 150 bp of 5' promoter region was amplified from *E. coli* genome DNA using KAPA HiFi PCR Kit following the manufacturer's protocol, and the amplicon was linked into a linearized pBBR1MCS6Y expression vector (gifted by Dr. Thomas A. Ficht) by NEBuilder HiFi DNA assembly to generate the recombinant pBBR1MCS6Y-CpxR plasmid. To generate the site-mutated *cpxR* (G89A) in pBBR1MCS6Y expression vector, two DNA fragments that covered the whole *cpxR* gene with 20 bp overlap in the middle were amplified by PCR using pBBR1MCS6Y-CpxR plasmid as a template, in which a shared mutation (G89A) was introduced into the middle overlap region.

The two fragments and pBBR1MCS6Y expression vector were assembled to form pBBR1MCS6Y-CpxR(G89A) by NEBuilder HiFi DNA assembly. All PCR primers are listed in **Table S4**, and the cloned DNA fragments were sequenced to confirm the presence of engineered mutation and the absence of other PCR-generated mutations (Eurofins Genomics LLC).

Generating *cpxR* complementary bacterial strains. Three transgenic *E. coli* strains were generated by transforming the plasmid pBBR1MCS6Y, pBBR1MCS6Y-CpxR, or pBBR1MCS6Y-CpxR(G89A) into *cpxR* knockout *E. coli* strain 10800 (KEIO collection)[25]. These three plasmids all can express a chloramphenicol resistant protein and GFP, and the stable strains were selected by antibiotic chloramphenicol and confirmed by GFP expression. An HA tag was fused to the N-terminal of CpxR and CpxR (G89A), which allowed the detection of their protein expression by Western blot. All *E. coli* strains used in this study are listed in **Table S5**.

Stress response assay. Bacteria were grown in LB medium at 37 ℃ overnight, and 30 μg/mL of chloramphenicol was added in the LB medium for the bacteria carrying engineered plasmids. The overnight-cultured cells were inoculated in fresh LB medium with 1:500 dilution, and the bacteria grown until the early or mid-log phase ($OD_{600} \leq 0.6$). The concentration of the freshly cultured bacteria was adjusted to $OD_{600} = 0.1$, and then 1:100 diluted and inoculated in LB medium with different stress conditions in a 96-well plate. Bacteria growth was monitored by recording OD_{600} every 30 min for 16 h using a Cytation5 (BioTek) plate reader. The bacterial responses to H_2O_2 (0.25, 0.5, 1.0 μM) and sodium dodecyl sulfate (2.5, 5.0, 10.0%) were tested in LB medium. The same set of stress responses was also tested in M9 medium with 0.2% glucose[52], and the same procedure repeated.

CpxR G89A protein structure analysis. Based on the published *E. coli* CpxR crystal structure (PDB ID: 4UHK)[53], the protein structure of CpxR mutation G89A was analyzed and superimposed using the UCSF Chimera[54]. The protein is depicted as ribbons with interacting side chains depicted as sticks colored by element. A closer view of the magnesium binding site was displayed, which contains relevant residues involved in the magnesium interaction within 5.0 Angstroms radius around Magnesium atom (**Fig. S8**).

Conflicts of interest

There are no conflicts to declare.

Acknowledgements

References

1. M. W. Gray, G. Burger and B. F. Lang, *Science*, 1999, **283**, 1476-1481.
2. A. Moustafa, B. Beszteri, U. G. Maier, C. Bowler, K. Valentin and D. Bhattacharya, *Science*, 2009, **324**, 1724-1726.
3. T. Laloum, M. Baudin, L. Frances, A. Lepage, B. Billault-Penneteau, M. R. Cerri, F. Ariel, M.-F. Jardinaud, P. Gamas, F. de Carvalho-Niebel and A. Niebel, *The Plant Journal*, 2014, **79**, 757-768.
4. M. Scholz, D. Albanese, K. Tuohy, C. Donati, N. Segata and O. Rota-Stabelli, *Nat Commun*, 2020, **11**, 5235.
5. E. Lefoulon, O. Bain, B. L. Makepeace, C. d'Haese, S. Uni, C. Martin and L. Gavotte, *PeerJ*, 2016, **4**, e1840.
6. A. Pandey, S. L. Ding, Q. M. Qin, R. Gupta, G. Gomez, F. Lin, X. Feng, L. Fachini da Costa, S. P. Chaki, M. Katepalli, E. D. Case, E. J. van Schaik, T. Sidiq, O. Khalaf, A. Arenas, K. S. Kobayashi, J. E. Samuel, G. M. Rivera, R. C. Alaniz, S. H. Sze, X. Qian, W. J. Brown, A. Rice-Ficht, W. K. Russell, T. A. Ficht and P. de Figueiredo, *Cell host & microbe*, 2017, **21**, 637-649 e636.
7. S. Pandey, D. Tripathi, M. Khubaib, A. Kumar, J. A. Sheikh, G. Sumanlatha, N. Z. Ehtesham and S. E. Hasnain, *Frontiers in Cellular and Infection Microbiology*, 2017, **7**.
8. M. Marchetti, D. Capela, M. Glew, S. Cruveiller, B. Chane-Woon-Ming, C. Gris, T. Timmers, V. Poinsot, L. B. Gilbert, P. Heeb, C. Médigue, J. Batut and C. Masson-Boivin, *PLOS Biology*, 2010, **8**, e1000280.
9. M. Marchetti, A. Jauneau, D. Capela, P. Remigi, C. Gris, J. Batut and C. Masson-Boivin, *Mol Plant Microbe Interact*, 2014, **27**, 956-964.
10. A. J. Waite and W. Shou, in *Engineering and Analyzing Multicellular Systems: Methods and Protocols*, eds. L. Sun and W. Shou, Springer New York, New York, NY, 2014, DOI: 10.1007/978-1-4939-0554-6_2, pp. 27-38.
11. G. B. Mackaness *Journal of Experimental Medicine*, 1962, **116**, 381-406.
12. G. B. Mackaness *Journal of Experimental Medicine*, 1964, **120**, 105-120.
13. E. G. D. Murray, R. A. Webb and M. B. R. Swann, *The Journal of Pathology and Bacteriology*, 1926, **29**, 407-439.
14. A. E. Zoheir, G. P. Späth, C. M. Niemeyer and K. S. Rabe, *Small (Weinheim an der Bergstrasse, Germany)*, 2021, **17**, 2007166.
15. G. Zhang, Y. Chen, Q. Li, J. Zhou, J. Li and G. Du, *Bioresource Technology*, 2021, **337**, 125467.
16. L. M. Fidalgo and S. J. Maerkl, *Lab on a Chip*, 2011, **11**, 1612-1619.
17. P. S. Dittrich and A. Manz, *Nat Rev Drug Discov*, 2006, **5**, 210-218.
18. P. Yager, T. Edwards, E. Fu, K. Helton, K. Nelson, M. R. Tam and B. H. Weigl, *Nature*, 2006, **442**, 412-418.
19. A. Han, H. Hou, L. Li, H. S. Kim and P. de Figueiredo, *Trends in Biotechnology*, 2013, **31**, 225-232.
20. R. Rusconi, M. Garren and R. Stocker, *Annual Review of Biophysics*, 2014, **43**, 65-91.
21. T. S. Kaminski, O. Scheler and P. Garstecki, *Lab on a Chip*, 2016, **16**, 2168-2187.
22. M. Masi, E. Pinet and J. M. Pagès, *Antimicrob Agents Chemother*, 2020, **64**.

23. W. L. Hand and N. L. King-Thompson, *Antimicrob Agents Chemother*, 1986, **29**, 135-140.

24. R. C. Prokesch and W. L. Hand, *Antimicrob Agents Chemother*, 1982, **21**, 373-380.

25. T. Baba, T. Ara, M. Hasegawa, Y. Takai, Y. Okumura, M. Baba, K. A. Datsenko, M. Tomita, B. L. Wanner and H. Mori, *Mol Syst Biol*, 2006, **2**, 2006.0008.

26. N. Weatherspoon-Griffin, D. Yang, W. Kong, Z. Hua and Y. Shi, *J Biol Chem*, 2014, **289**, 32571-32582.

27. P. J. Pomposiello, M. H. Bennik and B. Demple, *J Bacteriol*, 2001, **183**, 3890-3902.

28. Y. Liu and H. Lu, *Current Opinion in Biotechnology*, 2016, **39**, 215-220.

29. S. N. Bhatia and D. E. Ingber, *Nature Biotechnology*, 2014, **32**, 760-772.

30. C. L. Cosma, P. N. Danese, J. H. Carlson, T. J. Silhavy and W. B. Snyder, *Mol Microbiol*, 1995, **18**, 491-505.

31. E. Mileykovskaya and W. Dowhan, *J Bacteriol*, 1997, **179**, 1029-1034.

32. S. L. Vogt and T. L. Raivio, *FEMS Microbiol Lett*, 2012, **326**, 2-11.

33. T. F. Mahoney and T. J. Silhavy, *J Bacteriol*, 2013, **195**, 1869-1874.

34. D. Erturk-Hasdemir, S. F. Oh, N. A. Okan, G. Stefanetti, F. S. Gazzaniga, P. H. Seeberger, S. E. Plevy and D. L. Kasper, *Proceedings of the National Academy of Sciences*, 2019, **116**, 26157.

35. P. de Figueiredo, T. A. Ficht, A. Rice-Ficht, C. A. Rossetti and L. G. Adams, *The American Journal of Pathology*, 2015, **185**, 1505-1517.

36. Q. Chai, L. Wang, C. H. Liu and B. Ge, *Cellular & Molecular Immunology*, 2020, **17**, 901-913.

37. K. Karikó, M. Buckstein, H. Ni and D. Weissman, *Immunity*, 2005, **23**, 165-175.

38. S.-I. Han, C. Huang and A. Han, *Lab on a Chip*, 2020, **20**, 3832-3841.

39. S. I. Han, C. Huang and A. Han, 2019.

40. S. Yigit, H. Wang, S.-I. Han, Y. Cho and A. Han, *Microfluidics and Nanofluidics*, 2020, **24**, 52.

41. H. Zhang, K. Anoop, C. Huang, R. Sadr, R. Gupte, J. Dai and A. Han, *Sensors and Actuators B: Chemical*, 2021, DOI: https://doi.org/10.1016/j.snb.2021.131180, 131180.

42. C. Huang, J. A. Wippold, D. Stratis-Cullum and A. Han, *Biomedical Microdevices*, 2020, **22**, 76.

43. S. W. Wingett and S. Andrews, *F1000Res*, 2018, **7**, 1338.

44. J. J. Davis, A. R. Wattam, R. K. Aziz, T. Brettin, R. Butler, R. M. Butler, P. Chlenski, N. Conrad, A. Dickerman, E. M. Dietrich, J. L. Gabbard, S. Gerdes, A. Guard, R. W. Kenyon, D. Machi, C. Mao, D. Murphy-Olson, M. Nguyen, E. K. Nordberg, G. J. Olsen, R. D. Olson, J. C. Overbeek, R. Overbeek, B. Parrello, G. D. Pusch, M. Shukla, C. Thomas, M. VanOeffelen, V. Vonstein, A. S. Warren, F. Xia, D. Xie, H. Yoo and R. Stevens, *Nucleic Acids Res*, 2020, **48**, D606-d612.

45. A. Bankevich, S. Nurk, D. Antipov, A. A. Gurevich, M. Dvorkin, A. S. Kulikov, V. M. Lesin, S. I. Nikolenko, S. Pham, A. D. Prjibelski, A. V. Pyshkin, A. V. Sirotkin, N. Vyahhi, G. Tesler, M. A. Alekseyev and P. A. Pevzner, *J Comput Biol*, 2012, **19**, 455-477.

46. T. Brettin, J. J. Davis, T. Disz, R. A. Edwards, S. Gerdes, G. J. Olsen, R. Olson, R. Overbeek, B. Parrello, G. D. Pusch, M.

Shukla, J. A. Thomason, R. Stevens, V. Vonstein, A. R. Wattam and F. Xia, *Scientific Reports*, 2015, **5**, 8365.

47. B. Langmead and S. L. Salzberg, *Nature Methods*, 2012, **9**, 357-359.

48. G. T. Marth, I. Korf, M. D. Yandell, R. T. Yeh, Z. Gu, H. Zakeri, N. O. Stitziel, L. Hillier, P. Y. Kwok and W. R. Gish, *Nature genetics*, 1999, **23**, 452-456.

49. J. J. Davis, S. Gerdes, G. J. Olsen, R. Olson, G. D. Pusch, M. Shukla, V. Vonstein, A. R. Wattam and H. Yoo, *Frontiers in Microbiology*, 2016, **7**.

50. R. Overbeek, R. Olson, G. D. Pusch, G. J. Olsen, J. J. Davis, T. Disz, R. A. Edwards, S. Gerdes, B. Parrello, M. Shukla, V. Vonstein, A. R. Wattam, F. Xia and R. Stevens, *Nucleic acids research*, 2014, **42**, D206-D214.

51. G. M. Boratyn, C. Camacho, P. S. Cooper, G. Coulouris, A. Fong, N. Ma, T. L. Madden, W. T. Matten, S. D. McGinnis, Y. Merezhuk, Y. Raytselis, E. W. Sayers, T. Tao, J. Ye and I. Zaretskaya, *Nucleic acids research*, 2013, **41**, W29-W33.

52. *Cold Spring Harb. Protoc.*, 2010, DOI: 10.1101/pdb.rec12295. .

53. A. E. Mechaly, S. Soto Diaz, N. Sassoon, A. Buschiazzo, J.-M. Betton and P. M. Alzari, *Structure*, 2017, **25**, 939-944.e933.

54. E. F. Pettersen, T. D. Goddard, C. C. Huang, G. S. Couch, D. M. Greenblatt, E. C. Meng and T. E. Ferrin, *J Comput Chem*, 2004, **25**, 1605-1612.

Gene Name*	Gene Description	Protein change
ybfC	Uncharacterized protein	Lys189fs
ygcQ	Electron transfer flavoprotein, alpha subunit YgcQ	Leu220Arg
tus	DNA replication terminus site-binding protein	Pro160Thr
N/A	core protein	Gln33Lys
N/A	core protein	Gln33Lys
rhsA	**Protein RhsA**	**Ala179Thr**
rhsA	Protein RhsA	Lys262Thr
cpxR	**Copper-sensing two-component system response regulator**	**Gly89Ala**
cpxA	Copper sensory histidine kinase	Val174Ala
cpxA	**Copper sensory histidine kinase**	**Arg191His**
N/A	FIG01269488 protein, clustered with ribosomal protein L32p	Gln154Leu
csgA	Major curli subunit precursor	Val118Phe
yiaA	Inner membrane protein YiaA	Ala88Thr
mtlA	PTS system, mannitol specific EIIABC component	Ser26Phe
N/A	Ferric hydroxamate outer membrane receptor FhuA	Val1_Leu2insValProLeu
pinQ/pinR	Serine recombinase, PinQ/PinR-type	Ala159Val
pinQ/pinR	Serine recombinase, PinQ/PinR-type	Arg3Gln
ynaE	Uncharacterized protein, YnaE family	Thr51Lys
gadA/B	Glutamate decarboxylase (EC 4.1.1.15)	Lys1_Asn2insAspLeuSerIleAsnLys
N/A	core protein	Lys189fs

Mutation type	G10	G20	G25
Deletion	37.5	0	0
Nonsynonymous	50	0	0
Nonsynonymous	100	62.5	100
Nonsynonymous	12.5	0	12.5
Nonsynonymous	87.5	75	75
Nonsynonymous	**0**	**12.5**	**25**
Nonsynonymous	0	12.5	12.5
Nonsynonymous	**0**	**25**	**87.5**
Nonsynonymous	0	50	0
Nonsynonymous	**0**	**62.5**	**87.5**
Nonsynonymous	100	87.5	87.5
Nonsynonymous	100	87.5	87.5
Nonsynonymous	25	0	0
Nonsynonymous	50	0	0
Insertion	25	12.5	12.5
Nonsynonymous	50	50	37.5
Nonsynonymous	50	37.5	25
Nonsynonymous	62.5	50	50
Insertion	12.5	0	25
Insertion	0	12.5	12.5